

## Identification of dynamic characteristics of structures using vector backward auto-regressive model

Chen-Far Hung<sup>†</sup>, Wen-Jiunn Ko<sup>‡</sup> and Yen-Tun Peng<sup>‡†</sup>

*Department of Engineering Science and Ocean Engineering, National Taiwan University, Taipei, 106, Taiwan*

*(Received April 30, 2002, Accepted February 24, 2003)*

**Abstract.** This investigation presents an efficient method for identifying modal characteristics from the measured displacement, velocity and acceleration signals of multiple channels on structural systems. A Vector Backward Auto-Regressive model (VBAR) that describes the relationship between the output information in different time steps is used to establish a backward state equation. Generally, the accuracy of the identified dynamic characteristics can be improved by increasing the order of the Auto-Regressive model (AR) in cases of measurement of data under noisy circumstances. However, a higher-order AR model also induces more numerical modes, only some of which are the system modes. The proposed VBAR model provides a clear characteristic boundary to separate the system modes from the spurious modes. A numerical example of a lumped-mass model with three DOFs was established to verify the applicability and effectiveness of the proposed method. Finally, an offshore platform model was experimentally employed as an application case to confirm the proposed VBAR method can be applied to real-world structures.

**Key words:** vector backward auto-regressive model (VBAR); modal identification; offshore platform model; finite element method; experimental dynamics.

---

### 1. Introduction

Modal parameters, including natural frequencies, damping ratios and mode shapes, govern the dynamic behavior of a structural system. Obtaining accurately the modal parameters from test data is key in applying vibration control, and monitoring and detecting structural failures. Li and Ko (1987) used the Auto-Regressive Moving Average (ARMA) model to estimate the system modes for detecting and monitoring the structural failure of an offshore platform. Li *et al.* (1993) employed a Vector Auto-Regressive (VAR) model to estimate the modal parameters of ship structures. Viero and Roitman (1999) employed the structural parameter identification method to detect the damage of offshore platforms. Bernitsas and Suryatama (1999) used the large admissible perturbations with mode compensation to solve redesign problems to meet the requirements related to natural frequencies and mode shapes of offshore structures.

---

<sup>†</sup> Professor

<sup>‡</sup> Associate Professor

<sup>‡†</sup> Ph.D. Student

Many methods for modal identification have been developed over the last three decades. The modal identification methods can be categorized into time-domain and frequency-domain methods according to the processing domain. Frequency-domain methods, such as the FFT-based method (Cooley and Turkey 1965), are popular and predominant in engineering practice today. However, the closely spaced modes may not be easily recognized if the resolution of the frequency is not sufficiently high.

The time-domain methods are particularly useful for many modes in a multi-channels measurement system, or in the case of closely spaced and non-proportional modes. Ibrahim's time-domain method (Ibrahim and Mikulcik 1973), the complex exponential method (Ewins 1984), and the Eigen-system Realization Algorithm (ERA) (Juang and Pappa 1985) are well-known time-domain approaches developed from 1970s to the mid-1990s. The time series models, such as the ARMA model and the AR model, are also useful approaches for identifying the modal parameters of structures. The ARMA model is computationally complicated and the estimation of system parameters may be unstable. A higher-order AR model in place of the ARMA model (Kay 1988) can overcome this difficulty. Hung *et al.* (1998) developed a procedure based on the state equation of the VAR model to identify the modal parameters and frequency response function of structures in multiple output measurement system. Kumaresan and Tufts (1982) developed a backward prediction model to identify the natural frequencies and damping ratios of a dynamical system with a single channel measurement. In a common AR model, the output vector in the present step is predicted by the linear superposition of output vectors in previous steps. On the contrary, the proposed backward AR model can predict the present output vector from a linear combination of the future output vectors. Hollkamp and Batill (1991) developed a single-input and single-output backward ARMA model for parameter identification. Cooper (1992) employed the backward prediction error model to identify the natural frequencies and damping ratios, and pointed out that the backward model has the advantage of being able to distinguish system modes from spurious modes. The authors (Hung and Ko 2002) have investigated the basic characteristics of the modal identification method that uses the Vector Backward Auto-Regressive (VBAR) model, and the results reveal some advantages of the VBAR model.

In this paper, the VBAR model is applied to establish the state equation from the responses measured with multiple sensors on structures. The modal parameters of complex modes and normal modes of structures can be extracted from the system matrix of the identified state-space system, providing that the VBAR model is identified from the measured data.

## 2. Equations of motion

The motion of a structure with  $n$  DOFs under time-variant loading in configuration space can be expressed by the second-order differential equation for viscous damping,

$$M\ddot{z}(t) + \zeta\dot{z}(t) + Kz(t) = Fu(t) \quad (1)$$

where  $u(t) \in R^{r \times 1}$  and  $z(t) \in R^{n \times 1}$  are the force vector and the state vector, respectively;  $M$ ,  $\zeta$  and  $K \in R^{n \times n}$ , represent the mass, damping and stiffness matrices, respectively; the notation  $(\cdot)$  indicates differentiation with respect to time;  $F \in R^{n \times r}$  is the input influence matrix that characterizes the positions and types of inputs;  $r$  is the number of inputs.

For a measurement system that includes  $p$  sensors on a structure, the output equation that defines the relationship between the measured response,  $y(t) \in R^{p \times 1}$ , and the model response is,

$$y(t) = c_a \ddot{z}(t) + c_v \dot{z}(t) + c_d z(t) \quad (2)$$

where  $c_d$ ,  $c_v$  and  $c_a \in R^{p \times n}$ , are the output influence matrices of displacement, velocity and acceleration, respectively. The elements in matrices  $c_d$ ,  $c_v$  and  $c_a$  are Boolean parameters that specify the measured DOFs and the types of sensors.

A state vector that consists of displacement and velocity vectors is introduced:

$$x(t) = \begin{Bmatrix} z(t) \\ \dot{z}(t) \end{Bmatrix} \quad (3)$$

Eqs. (1) and (2) can be transformed into the state equation of motion and the output equation, respectively.

$$\dot{x}(t) = Ax(t) + Bu(t) \quad (4a)$$

$$y(t) = Cx(t) + Du(t) \quad (4b)$$

where  $A \in R^{2n \times 2n}$ ,  $B \in R^{2n \times r}$ ,  $C \in R^{p \times 2n}$  and  $D \in R^{p \times r}$  are the system matrix, the input matrix, the output matrix and the transmission matrix in the state space, respectively.

$$A = \begin{bmatrix} 0 & I \\ -M^{-1}K & -M^{-1}\zeta \end{bmatrix}, \quad B = \begin{bmatrix} 0 \\ M^{-1}F \end{bmatrix} \quad (5a,b)$$

$$C = [c_d \quad -c_a M^{-1}K \quad c_v \quad -c_a M^{-1}\zeta], \quad D = c_a M^{-1}F \quad (5c,d)$$

A discrete-time state equation of motion and output equation can be obtained through the sampling procedure with a sampling time interval  $\Delta t$ .

$$x_{k+1} = A'x_k + B'u_k \quad (6a)$$

$$y_k = Cx_k + Du_k \quad (6b)$$

where  $A' = e^{A\Delta t}$  and  $B' = (A' - I)A^{-1}B$ . The subscript  $k$  is the integer time index in time step  $t = k\Delta t$ .

### 3. Vector backward auto-regressive model

For a structure with  $p$  measured output channels and  $N$  data points in each channel, the output vector in time step  $k$  can be expressed as a linear superposition of the output vectors in next  $q$  time steps:

$$y_k = \sum_{i=1}^q a_i y_{k+i} + \varepsilon_k, \quad k = 1, \dots, N \quad (7)$$

where  $a_i \in R^{p \times p}$  and  $\varepsilon_k \in R^{p \times 1}$  are the parameter matrices and the error vector, respectively. Eq. (7) is a  $q$ -order VBAR model that consists of  $p$ -channels, and is represented by VBAR ( $p, q$ ). The parameter matrices of the VBAR model specify the pivotal dynamical characteristics of the structural systems. Eq. (7) can be expanded from time steps 1 to  $N - q$  and expressed in a compact matrix form,

$$\mathbf{Y} = \bar{\mathbf{a}} \mathbf{W} + \bar{\boldsymbol{\varepsilon}} \quad (8)$$

where  $\mathbf{Y} \in R^{p \times (N-q)}$  is the output matrix that consists of output vectors from time steps 1 to  $N - q$ ;  $\bar{\mathbf{a}} \in R^{p \times pq}$ ,  $\mathbf{W} \in R^{pq \times (N-q)}$  and  $\bar{\boldsymbol{\varepsilon}} \in R^{p \times (N-q)}$  are the VBAR coefficient matrix, the output data matrix and the error matrix, respectively.

$$\mathbf{Y} = [y_1 \ y_2 \ \dots \ y_{N-q}], \quad \mathbf{W} = \begin{bmatrix} y_2 & y_3 & \dots & y_{N-q+1} \\ y_3 & y_4 & \dots & y_{N-q+2} \\ \vdots & \vdots & \ddots & \vdots \\ y_{q+1} & y_{q+2} & \dots & y_N \end{bmatrix} \quad (9a,b)$$

$$\bar{\mathbf{a}} = [a_1 \ a_2 \ \dots \ a_q], \quad \bar{\boldsymbol{\varepsilon}} = [\varepsilon_1 \ \varepsilon_2 \ \dots \ \varepsilon_{N-q}] \quad (9c,d)$$

The VBAR coefficient matrix can be computed by the least squares method and expressed as follows.

$$\bar{\mathbf{a}} = \mathbf{Y} \mathbf{W}^\dagger \quad (10)$$

where  $\mathbf{W}^\dagger$  is the Moore-Penrose pseudo-inverse of  $\mathbf{W}$ .

A state vector  $x_k \in R^{pq \times 1}$ , consisting of  $q$  time steps of output vectors, is defined as,

$$x_k = \begin{bmatrix} y_k \\ y_{k+1} \\ \vdots \\ y_{k+q-1} \end{bmatrix} \quad (11)$$

Both sides of Eq. (7) also can be expanded from time steps  $k$  to  $k + q - 1$  to establish a discrete backward state equation and output equation as follows.

$$x_k = A_d x_{k+1} + B_d \varepsilon_k \quad (12a)$$

$$y_k = C_d x_k + D_d \varepsilon_k \quad (12b)$$

where  $A_d \in R^{pq \times pq}$ ,  $B_d \in R^{pq \times p}$ ,  $C_d \in R^{p \times pq}$  and  $D_d \in R^{p \times p}$  are the discrete state system matrix, the input matrix, the output matrix and the transmission matrix, respectively. These are expressed as follows.

$$A_d = \begin{bmatrix} a_1 & \dots & a_{q-1} & a_q \\ I & \dots & 0 & 0 \\ \vdots & \ddots & \vdots & \vdots \\ 0 & \dots & I & 0 \end{bmatrix}, \quad B_d = \begin{bmatrix} I \\ 0 \\ \vdots \\ 0 \end{bmatrix} \quad (13a,b)$$

$$C_d = [\bar{a}A_d^{-1}], \quad D_d = [I - \bar{a}A_d^{-1}B_d] \quad (13c,d)$$

The eigenvalues of the backward state equation can be determined by the characteristic polynomial of system matrix  $A_d$  (Gohberg 1982),

$$\lambda^q I - a_1 \lambda^{q-1} \dots - a_{q-1} \lambda - a_q = 0 \quad (14)$$

If all the eigenvalues of Eq. (14) are arranged in descending order, then,

$$|\lambda_i| \geq 1.0, \quad i = 1 \text{ to } 2n \quad (15a)$$

$$|\lambda_i| < 1.0, \quad i = 2n + 1 \text{ to } pq \quad (15b)$$

The first  $2n$  eigenvalues, which are  $n$  pairs of conjugate complex variables, are the system modes, and the leftover eigenvalues are spurious modes.

A complex  $z$ -plane is defined by a real horizontal axis and an imaginary vertical axis. If the  $pq$  eigenvalues determined from Eq. (14) are placed on the  $z$ -plane, then the eigenvalues located outside or on the unit circle are the system modes, and those inside the unit circle are the spurious modes. The unit circle of the  $z$ -plane plays a significant role as a characteristic boundary to separate the system modes from the spurious modes.

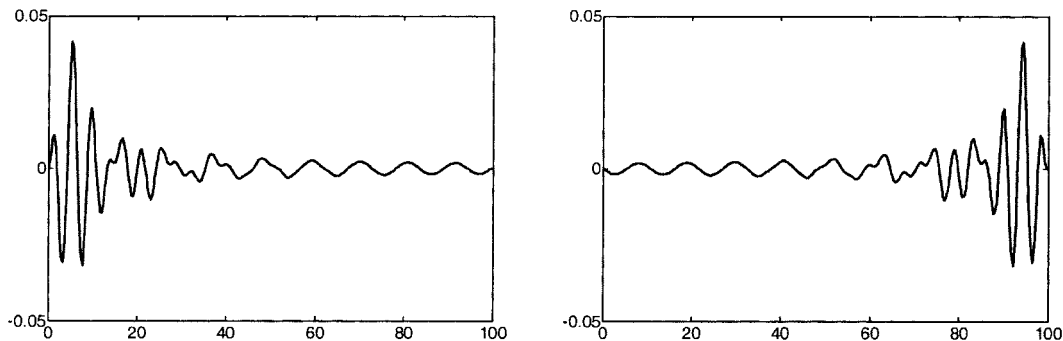


Fig. 1(a) Forward time series, (b) Backward time series

Fig. 1(a) and 1(b) show the time history of a measured acceleration in the forms of forward and backward time series, respectively. The forward time series of the system response is convergent, and the backward time series is divergent. Noise is essentially random and is non-divergent for both forward and backward time series. The magnitudes of all eigenvalues in the common forward AR model are less than or equal to one. However, for the BAR model, the magnitudes of the eigenvalues of system modes are greater than or equal to one, and for non-system modes are less than one.

### 3.1 Reduction of discrete state space model

The number of DOFs of a continuous structure is theoretically infinite. In practice, the sampling rate and the bandwidth of analysis are limited. The number of system modes of a dynamical measurement system is assumed to be  $n$ . If the measurement system has  $p$ -channels, then the number of eigenvalues of the VBAR ( $p, q$ ) model is the product of  $p$  and  $q$ ,  $pq$ . The order of the VBAR model,  $q$ , should be selected such that  $pq$  greatly exceeds  $2n$  to obtain the accuracy modal parameters in noisy measurement circumstances. The surplus  $pq - 2n$  spurious eigenvalues must be removed because of the overspecified order of the VBAR model. Therefore, Eq. (12) must be reduced.

The system matrix in Eqs. (12a) and (13a) can be decomposed as,

$$A_d = \Psi \Gamma \Psi^{-1} \quad (16)$$

where  $\Psi$  is the eigenvector matrix that consists of  $pq$  eigenvectors, and  $\Gamma$  is the diagonal eigenvalue matrix of  $pq$  eigenvalues. The eigenvector and eigenvalue matrices can be partitioned according to the system modes and spurious modes as,

$$\Psi = \begin{bmatrix} \Psi_{ss} & \Psi_{sn} \\ \Psi_{ns} & \Psi_{nn} \end{bmatrix}, \quad \Gamma = \begin{bmatrix} \Gamma_s & 0 \\ 0 & \Gamma_n \end{bmatrix} \quad (17a,b)$$

where the subscripts “s” and “n” indicate the “system” parts with regard to the  $2n$  system modes and the “non-system” parts with regard to the  $pq - 2n$  spurious modes, respectively. The matrices  $B_d$ ,  $\Psi^{-1}B_d$  and  $C_d$  are also partitioned as,

$$B_d = \begin{bmatrix} B_{ds} \\ B_{dn} \end{bmatrix}, \quad \Psi^{-1}B_d = \begin{bmatrix} B_s \\ B_n \end{bmatrix} \quad (18a,b)$$

$$C_d = [C_{ds} \quad C_{dn}] \quad (19)$$

The reduced discrete backward state space model, corresponding to the system modes, is expressed as,

$$x_k = A_r x_{k+1} + B_r \varepsilon_k \quad (20a)$$

$$y_k = C_r x_k + D_r \varepsilon_k \quad (20b)$$

where  $A_r \in R^{2n \times 2n}$ ,  $B_r \in R^{2n \times p}$ ,  $C_r \in R^{p \times 2n}$  and  $D_r \in R^{p \times p}$  are the reduced state system matrix, the input matrix, the output matrix and the transmission matrix, respectively. They are,

$$A_r = \Psi_{ss} \Gamma_s \Psi_{ss}^{-1}, \quad B_r = \Psi_{ss} B_s \tag{21a,b}$$

$$C_r = C_{ds} + C_{dn} \Psi_{ns} \Psi_{ss}^{-1}, \quad D_r = D_d \tag{21c,d}$$

The reduced discrete backward model can be transformed into a forward state space model as,

$$x_{k+1} = \bar{A}_r x_k + \bar{B}_r \epsilon_k \tag{22a}$$

$$y_k = \bar{C}_r x_k + \bar{D}_r \epsilon_k \tag{22b}$$

where  $\bar{A}_r$ ,  $\bar{B}_r$ ,  $\bar{C}_r$  and  $\bar{D}_r$  are expressed as follows.

$$\bar{A}_r = A_r^{-1}, \quad \bar{B}_r = -A_r^{-1} B_r \tag{23a,b}$$

$$\bar{C}_r = C_r A_r^{-1}, \quad \bar{D}_r = D_r - C_r A_r^{-1} B_r \tag{23c,d}$$

Eq. (22) is the equivalent system of Eq. (6).

### 3.2 Extraction of the normal modes

The matrix pair  $\langle \bar{A}_r, \bar{C}_r \rangle$  described by Eqs. (23a) and (23c) can be converted into continuous matrix pair  $\langle \bar{A}, \bar{C} \rangle$ , as follows,

$$\bar{A} = \ln(\bar{A}_r) / \Delta t, \quad \bar{C} = \bar{C}_r \tag{24a,b}$$

The identified matrix pair  $\langle \bar{A}, \bar{C} \rangle$  and the matrix pair  $\langle A, C \rangle$  in Eqs. (5a) and (5c) have the same dynamic characteristics in the case of noise-free system. The identified system matrix  $\bar{A}$  can be partitioned as,

$$\bar{A} = \begin{bmatrix} \bar{A}_{11} & \bar{A}_{12} \\ \bar{A}_{21} & \bar{A}_{22} \end{bmatrix} \tag{25}$$

The sub-matrices  $\bar{A}_{11}$  and  $\bar{A}_{12}$  generally are not null matrix and identity matrix, respectively. The complex modes can be calculated from the matrix pair  $\langle \bar{A}, \bar{C} \rangle$ . A nonsingular transformation matrix can be used to extract the normal modes in the same form as the pair  $\langle A, C \rangle$ . The transformation matrix is, (Hung *et al.* 2002)

$$T = \begin{bmatrix} c_d \bar{C} + c_v \bar{C} \bar{A}^{-1} + c_a \bar{C} \bar{A}^{-2} \\ c_d \bar{C} \bar{A} + c_v \bar{C} + c_a \bar{C} \bar{A}^{-1} \end{bmatrix} \tag{26}$$

Then, the transformed matrix pair  $\langle A^*, C^* \rangle$  can be expressed as follows.

$$A^* = T\bar{A}T^{-1}, \quad C^* = \bar{C}T^{-1} \quad (27a,b)$$

where,

$$A^* = \begin{bmatrix} 0 & I \\ -(M^{-1}K)^* & (M^{-1}\zeta)^* \end{bmatrix} \quad (28)$$

The lower-left partition of  $A^*$  is the equivalent of  $-M^{-1}K$  in the system matrix of Eq. (5a), and can be used to extract the normal modes.

### 3.3 Algorithm of modal identification by VBAR model

The procedures of the proposed method can be summarized as follows.

- (1) A VBAR ( $p, q$ ) model is established from measured data. The parameter matrices of the VBAR model are calculated using the least square method. See Eqs. (8) to (10).
- (2) A discrete backward state equation is established by expanding the  $q$ -time steps of output vectors in the VBAR model. See Eqs. (11) to (13).
- (3) The eigenvalues and eigenvectors of the discrete system matrix,  $A_d$ , are calculated by Eq. (16). Then, the system modes are separated from spurious modes by Eq. (15).
- (4) The discrete state space model is reduced to a lower order model that corresponds to the system modes. See Eqs. (20) to (21).
- (5) The reduced backward state space model is transformed into an equivalent forward discrete-time state equation of motion, and an output equation. See Eqs. (22) to (23).
- (6) The equivalent forward discrete-time state model is transformed into a continuous state space model. See Eq. (24)
- (7) The complex modes can be calculated from matrix  $\bar{A}$ . See Eq. (24a).
- (8) The identified matrix pair  $\langle \bar{A}, \bar{C} \rangle$  is transformed into the equivalent matrix pair  $\langle A^*, C^* \rangle$ . See Eqs. (26) to (27).
- (9) The normal modal parameters can be extracted from the equivalent  $(M^{-1}K)^*$ . See Eq. (28).

## 4. Examples

A numerical example and an experimental example are considered to illustrate the feasibility of the proposed method to identify the modal parameters of structures. The Modal Assurance Criteria (MAC) (Allemang and Brown 1983) is used to check the correlation between the identified mode shape  $\phi_{ei}$  and the analytical mode shape  $\phi_{ai}$ . It is defined as,

$$(\text{MAC})_i = \frac{|\phi_{ai}^T \phi_{ei}|^2}{(\phi_{ai}^T \phi_{ai})(\phi_{ei}^T \phi_{ei})}, \quad i = 1, \dots, n. \quad (29)$$

The value of the MAC is between zero and one. When the two mode shapes are consistent, the

resultant value of MAC is close to unity. In contrast, when two mode shapes are uncorrelated, the resultant MAC value is nearly zero.

4.1 Numerical simulation for a lumped-mass system with three DOFs

Fig. 2 shows a lumped-mass dynamic system with three DOFs. Table 1 shows the mass, damping and stiffness matrices of this model. The damping matrix is assumed to be non-Rayleigh damping. Modal parameters were identified in the free vibration case. The initial displacements of the three DOFs are set to: [0, 0, 0.1]. The sampling frequency, 3 Hz, is selected to be approximately ten times the maximum natural frequency of the system with three DOFs. The number of data points

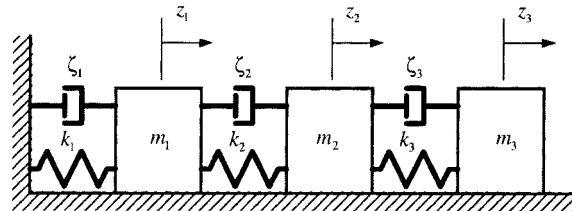


Fig. 2 A lumped-mass dynamic system with three DOFs

Table 1 Mass, damping, and stiffness matrices in the three DOFs model

Mass matrix [M]	Damping matrix [ζ]	Stiffness matrix [K]
$\begin{bmatrix} 3 & 0 & 0 \\ 0 & 2 & 0 \\ 0 & 0 & 1 \end{bmatrix}$	$\begin{bmatrix} 0.1 & -0.1 & 0 \\ -0.1 & 0.3 & -0.2 \\ 0 & -0.2 & 0.2 \end{bmatrix}$	$\begin{bmatrix} 6 & -2 & 0 \\ -2 & 3 & -1 \\ 0 & -1 & 1 \end{bmatrix}$

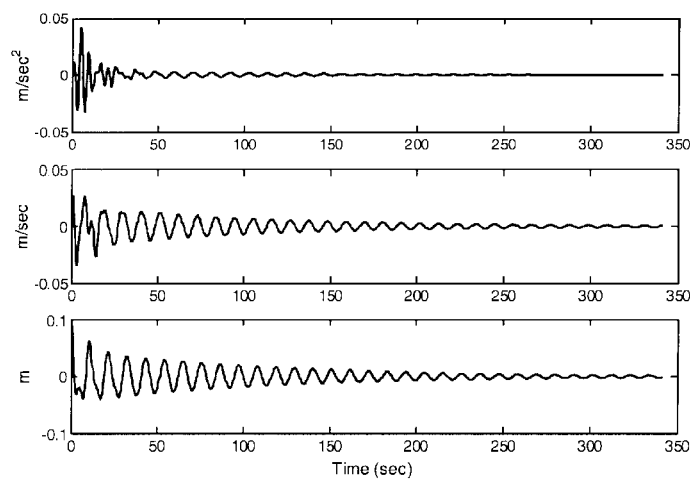


Fig. 3 Time history responses of 3 DOFs model

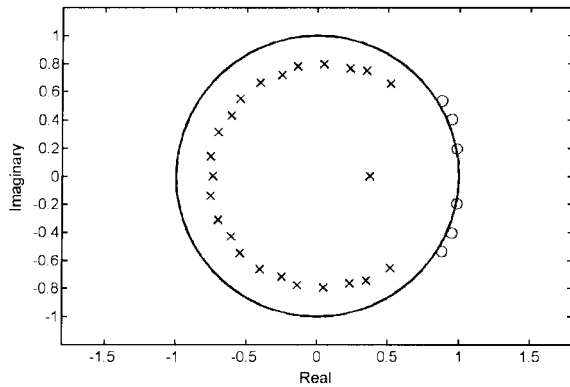


Fig. 4 Distribution of eigenvalues for VBAR(3,10) model

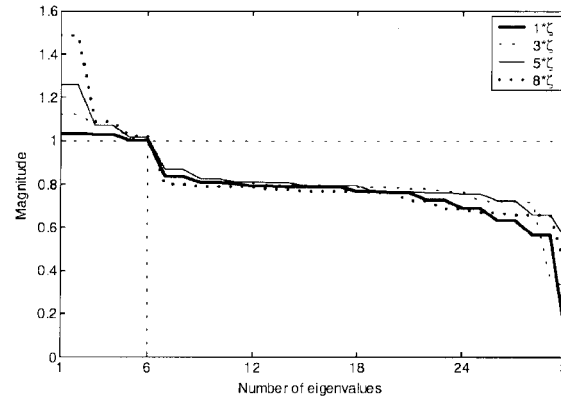


Fig. 5 Magnitudes of eigenvalues at various damping levels

associated with each DOF is 1024. The acceleration, velocity, and displacement responses at  $m_1$ ,  $m_2$  and  $m_3$  were simulated to elucidate the availability in the case of combined measurements. Fig. 3 shows time histories at various positions.

The VBAR (3,10) model is initially selected to illustrate the separation of system modes from spurious modes, and thereby to demonstrate the advantage of the proposed method in the selection of system modes. Fig. 4 shows the distribution of the 30 eigenvalues of the model. Symbols 'o' and 'x' indicate the system and spurious eigenvalues, respectively. The figure shows clearly that six system eigenvalues are outside the unit circle.

The modal identifications under noise-free conditions for a system with 1-, 3-, 5- and 8-times the damping matrix,  $\zeta$ , in Table 1 were examined to show the effect of the damping level on the identified results. Fig. 5 presents the magnitudes of all 30 eigenvalues at various damping levels. The magnitudes of the first six eigenvalues of the system at various damping levels are greater than one, so the number of vibration modes is easily identified as three. Clearly also, the magnitudes of the system eigenvalues in a heavily damped system exceed those of a lightly damped system. Hence, the eigenvalues are farther from the unit circle for a more heavily damped system. Consequently, the extraction of the system modes of a heavily damped system is easier than that of a lightly damped system.

The effect of various noise levels on the estimation of modal parameters is checked to show the proposed approach can be applied to a real-world structure. The noise is assumed to be a white noise with zero mean and various variances of 3%, 6% and 10% of the maximum responses. When the noise level increases, the order of VBAR model must be increased to yield accurate results. The VBAR model with orders 5, 20, 40 and 60 are selected for noise levels of 0%, 3%, 6% and 10%, respectively. Table 2 lists the identified modal parameters at various noise levels. The results indicate that the identified modal parameters are very consistent with the exact solution at various noise levels.

#### 4.2 Experimental modal identification of an offshore platform model

A 1:18.4 scale model of an offshore platform shown in Fig. 6 is considered as an experimental

Table 2 Identified eigenvalues, natural frequencies, damping ratios and MAC values at various noise levels

	Mode	Eigenvalues	Natural frequencies (Hz)	Damping ratios (%)	MAC
Exact	1	$-0.0093 \pm 0.5839i$	0.0928	0.0159	
	2	$-0.0953 \pm 1.2040i$	0.1911	0.0789	
	3	$-0.0871 \pm 1.6349i$	0.2624	0.0532	
0% noise VBAR (3,5)	1	$-0.0093 \pm 0.5839i$	0.0928	0.0159	1.0000
	2	$-0.0953 \pm 1.2040i$	0.1911	0.0789	1.0000
	3	$-0.0871 \pm 1.6349i$	0.2624	0.0532	1.0000
3% noise VBAR (3,20)	1	$-0.0093 \pm 0.5840i$	0.0929	0.0159	1.0000
	2	$-0.0937 \pm 1.2043i$	0.1913	0.0776	1.0000
	3	$-0.0854 \pm 1.6356i$	0.2623	0.0522	0.9988
6% noise VBAR (3,40)	1	$-0.0092 \pm 0.5840i$	0.0928	0.0159	1.0000
	2	$-0.0926 \pm 1.2046i$	0.1910	0.0781	1.0000
	3	$-0.0833 \pm 1.6357i$	0.2631	0.0522	0.9945
10% noise VBAR (3,60)	1	$-0.0091 \pm 0.5836i$	0.0928	0.0157	1.0000
	2	$-0.0939 \pm 1.2057i$	0.1916	0.0777	0.9997
	3	$-0.0839 \pm 1.6363i$	0.2621	0.0512	0.9945

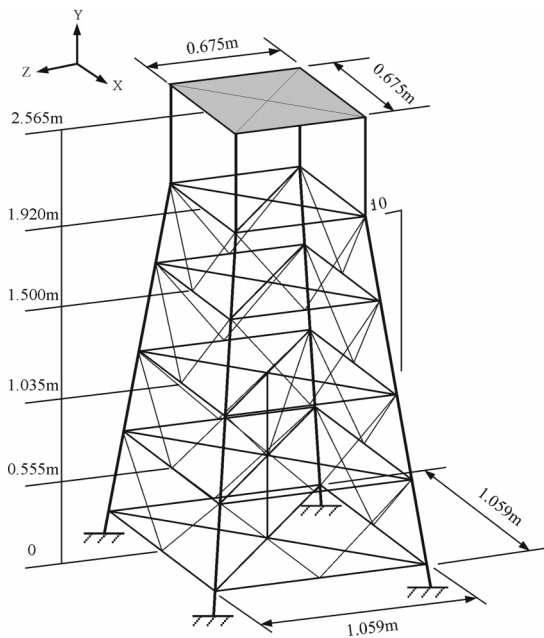


Fig. 6 1:18.4 scale model of a fixed platform

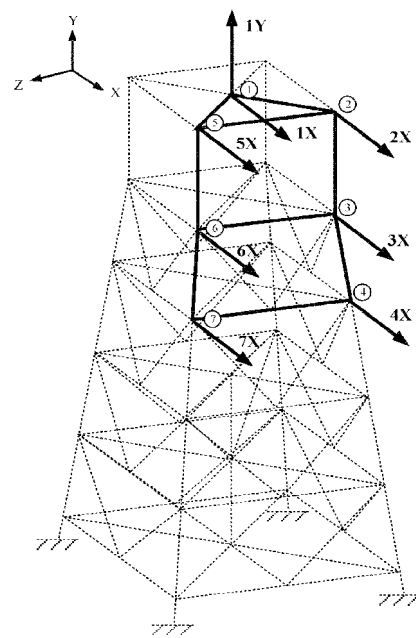


Fig. 7 Arrangement of the orientation and position of accelerometers on the platform

Table 3 Material and geometrical parameters of the platform model

Material properties	Young's modulus (MPa)	2.07e5	
	Density (kg/m <sup>3</sup> )	7809	
	Poission's ratio	0.3	
Geometric parameters	Top plate	Thickness (mm)	3
	Tube 1	Outer diameter (mm)	19.1
		Thickness (mm)	0.9
	Tube 2	Outer diameter (mm)	15.9
		Thickness (mm)	1.2
	Tube 3	Outer diameter (mm)	12.7
Thickness (mm)		1.2	

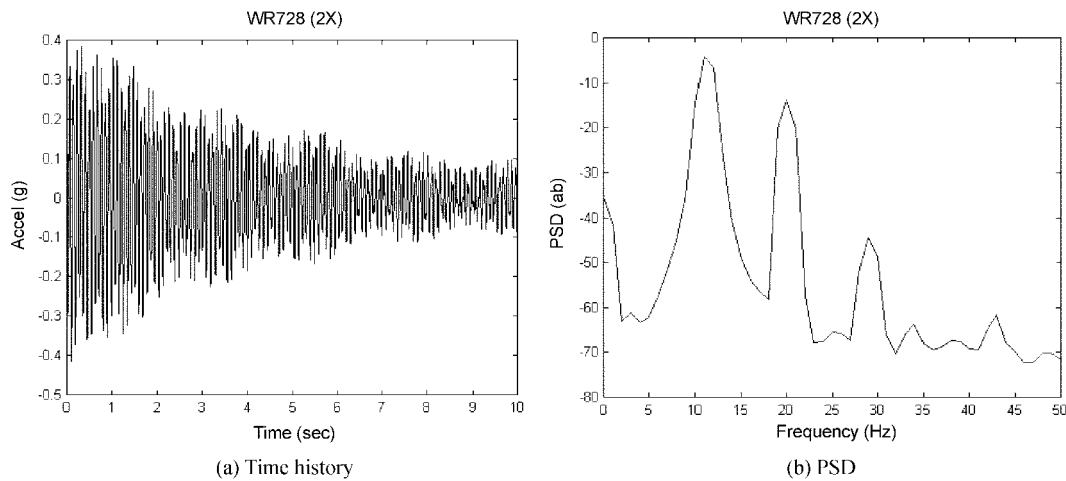


Fig. 8 Time history and PSD of measured acceleration from sensor 2X

case. The platform model is built of stainless steel tubes and a top-plate. Table 3 lists the geometric and material properties of the structural members. Tubes 1, 2 and 3 are used as vertical columns, horizontal beams and inclined braces, respectively. Fig. 7 depicts the arrangement of the orientation and the positions of the accelerometers on the platform structure.

A PCB impulse hammer was used to impact horizontally the top plate. The free response signals were collected by a multi-channels data acquisition system at a sampling frequency 100 Hz. The number of data per channel is 1024. Fig. 8 shows the time history and the Power Spectrum Density (PSD) of acceleration measured by sensor 2X. Fig. 8(b) shows three large peaks with frequencies of 10.9, 20 and 29 Hz. These peak frequencies correspond to the natural frequencies of the platform structure. The first two modes of the structure, at 10.869 and 11.204 Hz, cannot be identified only from the PSD diagram because of the limited frequency resolution.

A 3D-FEM modal analysis using the ANSYS package is carried out for comparison. Fig. 9

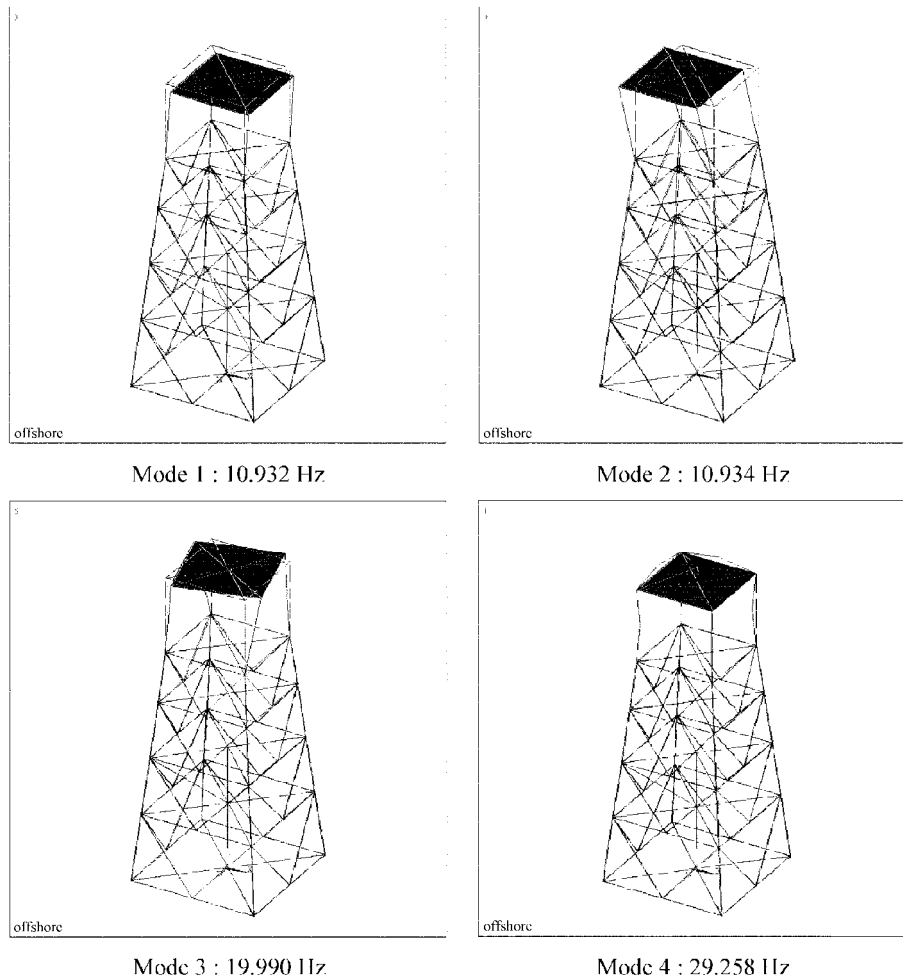


Fig. 9 Mode shapes calculated by FEM

Table 4 Comparison of modal parameters obtained by FEM and VBAR model

Mode	Vibration type	FEM	VBAR(8,30)		
		Frequency (Hz)	Frequency (Hz)	Damping ratio (%)	MAC
1	Bending-1	10.932	10.869	0.17	0.991
2	Bending-2	10.934	11.204	0.17	0.996
3	Torsion-1	19.990	19.784	0.49	0.973
4	Axial-1	29.258	28.986	0.38	0.995

shows the relative mode shapes of the first four modes calculated by FEM. The VBAR model of order 30 was used in this experimental case. Table 4 shows the modal parameters obtained by FEM analysis and modal identification. The results of modal identification are similar to those of FEM,

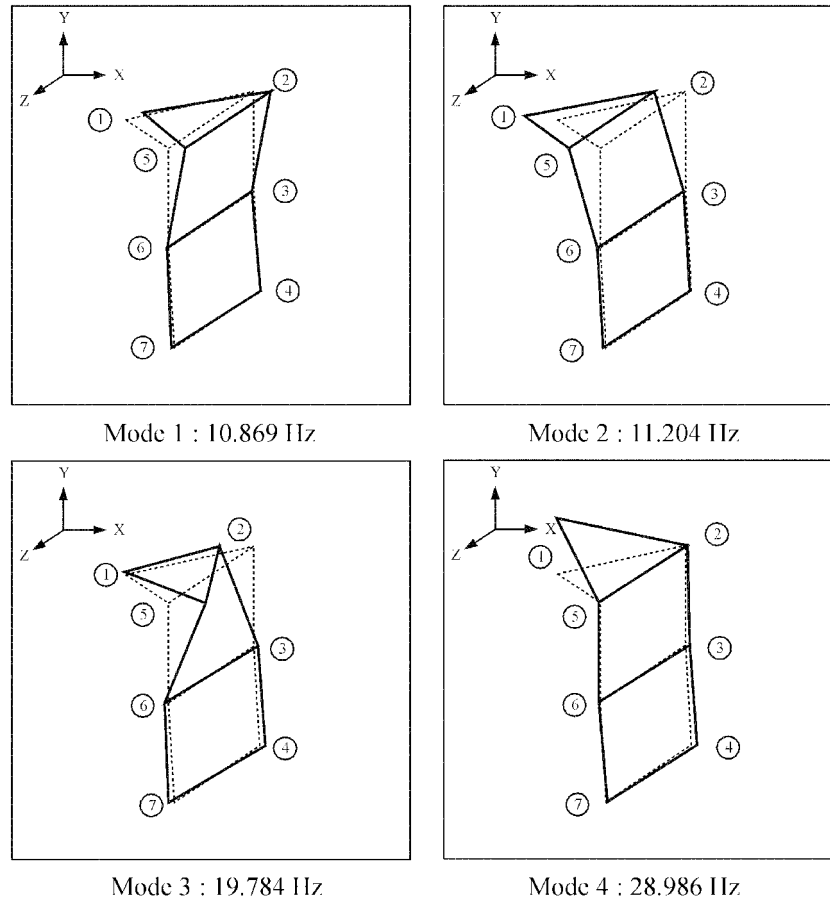


Fig. 10 Relative mode shapes identified by VBAR model

and the MAC values of the first four modes are higher than 0.97. Fig. 10 shows the identified relative mode shapes at measured DOFs. The results reveal that the identified natural frequencies and mode shapes of the four modes agree with those obtained by FEM analysis. Additionally, modal identification can approximately estimate the damping ratio, which cannot be estimated from a FEM package.

The global modes of platform structure on lower frequencies were considered in this case. The orientation, the position, the sampling rate, and the filtering bandwidth of the sensors were arranged for these modes. Only four modes are identified from the experimental data on the platform structure because of the restriction of the measurement bandwidth. The first four global mode shapes of top storey are relatively larger than those of lower storeys below 1.920 m (See Fig. 6), because the bottom of structure is constrained. However, the modes shapes of lower storeys may be larger than those of top storey in local modes or some global modes on higher frequencies.

## 5. Conclusions

This investigation has developed a VBAR model and its associated state space system for the identification of modal parameters from multi-channels response data. The proposed VBAR method accurately identifies not only the natural frequencies and damping ratios, but also the mode shapes. Under noisy measurement conditions, a higher-order VBAR model can improve the accuracy of the identified modal parameters. The proposed method provides a clear characteristic boundary to separate the system modes from the spurious modes. The extraction of system modes of a heavily damped system is easier than that of a lightly damped system.

The proposed method can also be applied to forced vibration cases, if the frequency bandwidth of the exciting force is sufficiently wide. The applications may be somewhat limited, if the exciting forces have narrow frequency bandwidths. A further study to prevent the spurious modes from exciting forces is under way.

## Acknowledgements

The authors would like to thank the National Science Council of the Republic of China for financially supporting this research under Contract No. NSC 90-2611-E-002-027.

## References

- Allemang, R.L. and Brown, D.L. (1983), "A correlation coefficient for modal vector analysis", *Proc. 1st Int. Modal Analysis Conf., Bethel, Connecticut, U.S.A.*, 110-116.
- Bernitsas, M.M. and Suryatama, D. (1999), "Structural redesign by large admissible perturbations with static mode compensation", *Journal of Offshore Mechanics and Arctic Engineering*, **121**, 39-46.
- Cooley, J.W. and Turkey, J.W. (1965), "An algorithm for the machine calculation of complex Fourier series", *Mathematics of Computation*, **19**, 297-301.
- Cooper, J.E. (1992), "The use of backwards model for structural parameters identification", *Mechanical System and Signal Processing*, **6**(3), 217-228.
- Ewins, D.J. (1984), *Modal Testing Theory and Practice*, Research Studies Press Ltd, London.
- Gohberg, I., Lancaster, P. and Rodman, L. (1982), *Matrix Polynomials*, Academic Press, New York.
- Hollkamp, J.J. and Batill, S.M. (1991), "Automated parameter identification and order reduction for discrete time series models", *AIAA J.*, **29**(1), 96-103.
- Ibrahim, S.R. and Mikulcik, E.C. (1973), "A time domain vibration test", *Shock and Vibration Bulletin*, **43**, part 4.
- Juang, J.N. and Pappa, R.S. (1985), "An eigensystem realization algorithm for modal parameter identification and model reduction", *Journal of Guidance, Control, and Dynamics*, **8**, 620-627.
- Hung, C.F., Ko, W.J. and Tai, C.H. (1998), "Identification of modal parameters by the state equation of vector auto-regressive model", (in Chinese), *Journal of the Society of Naval Architects and Marine Engineers, ROC*, **17**(3), 35-44.
- Hung, C.F., Ko, W.J. and Tai, C.H. (2002), "Identification of dynamic systems from data composed by combination of their response components", *Engineering Structures*, **24**, 1441-1450.
- Hung, C.F. and Ko, W.J. (2002), "Identification of modal parameters from measured output data using vector backward autoregressive model", *J. Sound and Vib.*, **256**(2), 249-270.
- Kay, S.M. (1988), *Modern Spectral Estimation - Theory & Application*, Prentice Hall, New Jersey.
- Kumaresan, R. and Tufts, D.W. (1982), "Estimating the parameters of exponentially damped sinusoids and

- pole-zero modeling in noise”, *IEEE Transactions on Acoustics, Speech, and Signal Processing*, **30**(6), 833-840.
- Li, C.S. and Ko, W.J. (1987), “On the application of the time series in structural failure detection and monitoring for offshore applications”, *The Royal Institution of Naval Architects*, **130**, 315-327.
- Li, C.S., Ko, W.J., Li, C.S. and Shyu, R.J. (1993), “Vector autoregressive modal analysis with application to ship structures”, *J. Sound and Vib.*, **167**(1), 1-15.
- Viero, P.F. and Roitman, N. (1999), “Application of some damage identification methods in offshore platforms”, *Marine Structures*, **12**, 107-126.